Systematic model development for partial nitrification of landfill leachate in a SBR

R. Ganigué, E. I. P. Volcke, S. Puig, M. D. Balaguer, J. Colprim and G. Sin

ABSTRACT

This study deals with partial nitrification in a sequencing batch reactor (PN-SBR) treating raw urban landfill leachate. In order to enhance process insight (e.g. quantify interactions between aeration, CO_2 stripping, alkalinity, pH, nitrification kinetics), a mathematical model has been set up. Following a systematic procedure, the model was successfully constructed, calibrated and validated using data from short-term (one cycle) operation of the PN-SBR. The evaluation of the model revealed a good fit to the main physical-chemical measurements (ammonium, nitrite, nitrate and inorganic carbon), confirmed by statistical tests. Good model fits were also obtained for pH, despite a slight bias in pH prediction, probably caused by the high salinity of the leachate. Future work will be addressed to the model-based evaluation of the interaction of different factors (aeration, stripping, pH, inhibitions, among others) and their impact on the process performance.

Key words | anammox, calibration, identifiability, modelling, partial nitrification, SBR

R. Ganigué (corresponding author)
M. D. Balaguer
J. Colprim
Laboratory of Chemical and Environmental Engineering (LEQUIA),
Institute of the Environment, University of Girona,
Campus Montilivi s/n, Facultat de Ciències,
E-17071 Girona, Catalonia,
Spain
E-mail: *ramon@lequia.udg.cat*;
marilos@lequia.udg.cat;
J.Colprim@lequia.udg.cat

E. I. P. Volcke
Department of Applied Mathematics,
Biometrics and Process Control, Ghent University,
Coupure links 653, 9000 Gent,
Belgium
E-mail: *eveline.volcke@ugent.be*

S. Puig
Catalan Institute for Water research (ICRA).
Parc Científic i Tecnològic de la Universitat de Girona, C/Emili Grahit, 101. Edifici H_2O,
E-17003 Girona, Catalonia,
Spain
E-mail: *spuig@icra.cat*

G. Sin
CAPEC-Department of Chemical and Biochemical Engineering, Technical University of Denmark,
Building 229, DK-2800 Kgs Lyngby,
Denmark
E-mail: *gsi@kt.dtu.dk*

INTRODUCTION

During partial nitrification, ammonium is oxidised to nitrite while further nitrification to nitrate is suppressed. This reaction plays an important role during biological nitrogen removal from streams with high ammonium concentrations (e.g. sludge digester supernatant, landfill leachate), when aiming at lower oxygen and organic matter consumption, in comparison with conventional nitrification/denitrification treatments. For instance, partial nitrification reactors can be coupled with an anammox process, ending up in a fully autotrophic system capable of removing high nitrogen loads in a more sustainable way (Van Dongen *et al.* 2001).

Previous studies (Lai *et al.* 2004; Ganigué *et al.* 2007) demonstrated the feasibility of achieving a successful nitritation using the Sequencing Batch Reactor (SBR) technology for the treatment of nitrogen high-loaded streams. However, despite the experience acquired, the reactor's response to changes in the operational conditions and influent characteristics is not always easy to understand or predict, given the complexity of the system, e.g. interactions between oxygen supply, CO_2 stripping, alkalinity, pH, inhibition effects, nitrification kinetics, among others.

Mathematical models can be a useful tool to increase the process knowledge and help to better understand

doi: 10.2166/wst.2010.979

biological processes and the physical phenomena taking place in a partial nitrification-sequencing batch reactor (PN-SBR). Traditional modelling has assumed nitrification and denitrification as single-step processes (Henze *et al.* 2000). Nevertheless, when modelling a partial nitrification system it is necessary to consider nitrite as an intermediary step of nitrification and denitrification. Nowadays there are several biological models describing nitrite build-up, as reviewed by Sin *et al.* (2008). Some of these models focus on the treatment of nitrogen high loaded-streams (Hellinga *et al.* 1999; Volcke *et al.* 2002; Wett & Rauch 2003; among others) and can be used as a basis when modelling specific processes. It is clear that existing models may need to be modified or extended to include all relevant physical-chemical processes and biochemical transformations for a given application. Besides, the model needs to be calibrated for influent and process specific parameters. This is highlighted in this study for partial nitrification of landfill leachate in a SBR, aiming at increased process knowledge (e.g. quantify interactions between aeration, CO_2 stripping, alkalinity, pH, nitrification kinetics) and focusing on the short-term dynamics (cycle basis). This work also deals with the usefulness of a systematic calibration guideline and its refinement.

MATERIALS AND METHODS

Reactor set-up and operation

The reactor under study concerns a 20 L lab-scale SBR treating raw urban landfill leachate. The reactor temperature was controlled at 36 ± 1°C through a water jacket. Dissolved oxygen was kept at a set-point value of 2.0 mg O_2 L^{-1} by an on-off controller acting on the airflow. The SBR was equipped with a monitoring and control system including on-line probes measuring dissolved oxygen (DO), pH, oxidation-reduction potential (ORP) and temperature (T). A more detailed description of the experimental set-up can be found in Ganigué *et al.* (2007).

The SBR was operated for more than 400 days with a constant cycle length of 8 h. During a first period (day 0 to 245), a fed-batch operating strategy was applied, characterised by one long feeding phase. Afterwards, the operation strategy was switched to a step-feeding, with multiple feeding events (days 245 to 410). Figure 1 presents both strategies in a schematic way.

After a transition period (of 58 and 27 days, respectively), each of these operational periods was characterised by fixed cyclic concentration profiles. The model calibration has been based on the steady-state profiles of the fed-batch phase, while the data of the step-feed phase have been used for model validation. During both phases, the nitrogen loading rate (NLR) was 1.3 kg N m^{-3} d^{-1}. Despite the variations in influent ammonium, the NLR was kept constant by adjusting the inflow, ending up in different hydraulic retention times (HRT) for each phase (fed-batch: HRT = 1.35 days; step-feed: HRT = 1.53 days). In both phases the sludge retention time (SRT) was around 3–5 days.

Calibration guideline

In order to perform the modelling procedure in a systematic and organised way, the guideline presented in Corominas (2006) for the SBR systems was followed. Nevertheless, due to specific features of the PN-SBR system, minor modifications were introduced to this guideline. These changes

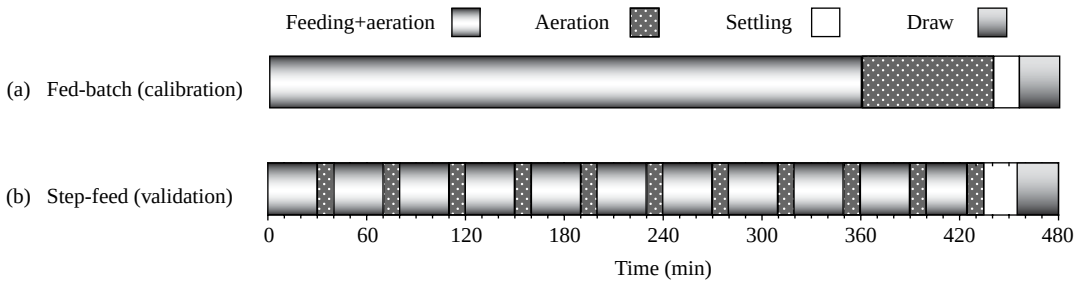

Figure 1 | SBR cycle definition in both periods. a) fed-batch and b) step-feed. (Ganigué *et al.* 2008).

included: (i) the adaptation of the influent wastewater characterisation to the available historical data, (ii) the inclusion of an identifiability analysis to find an identifiable parameter subset for model fine-tuning (Ruano *et al.* 2007) and (iii) the use of additional statistical tests for the evaluation of the model fits to data.

Wastewater characterisation

Four state variables involving nitrogen fractionation were considered in Corominas (2006): S_{NH} (linked to ammonium), S_{NO} (equivalent to the sum of nitrites and nitrates), and S_{ND} and X_{ND} (which accounted for the soluble and particulate nitrogen fractions of soluble and particulate organic matter, respectively). In our partial nitrification model, nitrite and nitrate are considered separately. On the other hand, S_{ND} and X_{ND} are not taken up, since organic nitrogen is considered as a fraction of the organic matter (S_S, S_I, X_S and X_I).

Regarding the organic matter, the available historical data sets did not contain soluble chemical oxygen demand (COD_S) measurements, essential for the organic matter fractionation. Nevertheless, dissolved organic carbon (DOC) measurements were available. In this way, COD_S at the influent and effluent were calculated from the DOC values, applying empirical ratios. These ratios were experimentally found to be 1.86 mg COD_S per mg DOC at the influent, and 2.3 mg COD_S per mg DOC at the effluent.

Identifiability analysis

The methodology defined in Brun *et al.* (2002), based on a local sensitivity analysis, was used to find an identifiable subset of parameters to calibrate the PN-SBR model. To be identifiable, a parameter subset has to fulfil two conditions. First, a model output, y, has to be sufficiently sensitive to individual changes of each parameter, j. This is addressed by the sensitivity measure δ_{yj}^{msqr}. Secondly, variations in the model output due to changes in single parameters may not be approximately cancelled by appropriate changes in other parameters. This analysis of the parameter interdependences is addressed by the collinearity index, γ_K. The determinant value, ρ_K, takes into account both identifiability conditions simultaneously and is, therefore, particularly suited for the assessment of identifiability of parameter subsets. The identifiability analysis has been carried out following the different steps gathered in Table 1.

Statistical tests for model evaluation

To support the visual evaluation, the quality of the fits was assessed also by statistical tests (Table 2, see Power 1993).

MAE and RMSE are statistical tests directly related to each output, accounting for the same units. On the other hand, ARD is a test that informs about relative deviations. Finally, the Janus coefficient measures the predictive accuracy of the model, and its value should be close to 1.

Table 1 | Different steps of the identifiability methodology of Brun *et al.* (2002)

Non-dimensional sensitivity (S_{ij})	Sensitivity measure (δ_{yj}^{msqr})	Collinearity index (γ_K)	Determinant value (ρ_K)
$S_{ij} = \frac{\partial y_i}{\partial \theta_j} \cdot \frac{\theta_j}{y_i}$	$\delta_{yj}^{msqr} = \sqrt{\frac{1}{n}\sum_{i=1}^{n} S_{ij}^2}$	$\gamma_K = \frac{1}{\sqrt{\min \bar{\lambda}_k}}$	$\rho_K = \det\left(S_K^T S_K\right)^{1/2k}$

where $\delta y_i/\delta\theta_j$ is defined as the absolute sensitivity of the model output y_i to the parameter θ_j; n the number of measurements (at different time instants); min $\bar{\lambda}_k$ is the smallest eigenvalue of the normalised subset matrix $\bar{S}_K^T \bar{S}_K$, and $\det\left(S_K^T S_K\right)^{1/2k}$ is the determinant function of the $n \times K$ subset matrix of S.

Table 2 | Statistical tests

Mean absolute error (MAE)	Root mean squared error (RMSE)	Average relative deviation (ARD)	Janus coefficient (J^2)
$MAE = \frac{1}{n}\sum_{i=1}^{n} \lvert y_{meas,i} - y(t_i)\rvert$	$RMSE = \sqrt{\frac{1}{n}\sum_{i=1}^{n} (y_{meas,i} - y(t_i))^2}$	$ARD = \sqrt{\frac{1}{n}\sum_{i=1}^{n} \left(\frac{\lvert y_{meas,i} - y(t_i)\rvert}{y_{meas,i}}\right)}$	$J^2 = \frac{\frac{1}{n\_val}\sum_{i=1}^{n\_val} (y_{meas,i} - y(t_i))^2}{\frac{1}{n\_cal}\sum_{i=1}^{n\_cal} (y_{meas,i} - y(t_i))^2}$

n is the total number of observations of the variable y; $y_{meas,i}$ is the ith measurement of the variable y, and $y(t_i)$ is the corresponding model output at time i; n_cal and n_val are the total number of measurements in calibration and validation period, respectively.

THE PARTIAL NITRIFICATION MODEL

The partial nitrification SBR model (implemented in Matlab-Simulink®) was based on the SHARON model developed by Volcke *et al.* (2002). This model was adapted from state variables expressed on a molar basis to the same units as the Activated Sludge Models (ASM, Henze *et al.* 2000). Firstly, the hydraulic model was changed from a continuous stirred-tank reactor (CSTR) to a SBR, by implementing a cycle that was repeated over time. Biological reactions took place during feeding and reaction phases. Settling and draw phases were ideally modelled, assuming that no biological reactions were taking place. Furthermore, settling was modelled considering the SBR as a point settler. The total suspended solids in the effluent were assumed to be the non-settlable fraction (f_{ns}).

Regarding the biokinetic model (given as appendix in matrix format), reversible inhibition kinetics were included for free ammonia and free nitrous acid for both ammonium and nitrite oxidation processes (the original model only contained nitrous acid inhibition of ammonium oxidation). In addition, bicarbonate limitation was taken up. Focusing on the heterotrophic conversions, a general readily biodegradable organic matter component (S_S) was considered as a substrate for heterotrophic biomass, instead of methanol. Besides, the following biokinetic conversions were added: hydrolysis of the slowly biodegradable organic matter and the endogenous respiration processes (nine in total) of each biomass type (X_{AOB}, X_{NOB}, X_H) on each possible electron acceptor (O_2, NO_2^- and NO_3^-). As a result, this model considers 15 different microbial transformation processes, all taking place in the liquid phase. The stoichiometry and kinetics for the biological conversion reactions can be found in the appendix (Table A.1), as well as the kinetic and stoichiometric parameters (Tables A.2 and A.3). Temperature dependency was also taken into account on the kinetic parameters by an Arrhenius type expression, despite the reactor being operated at a constant temperature. In this way, temperature correction coefficients are also included in the appendix (Table A.4).

Besides the reactor liquid phase, in which the biological reactions take place, the model also considers a gas phase (i.e. the bubbles in the liquid phase). Between these phases, which are both assumed to be perfectly mixed, transport of oxygen, carbon dioxide, nitrogen and ammonia occurs. Volcke *et al.* (2002) did not take up interphase transport (stripping) of ammonia, but it is considered in this study due to the very high influent concentration of ammonium (about $2\,g\,N\,L^{-1}$).

Nitrification of wastewater streams with high ammonium concentrations combined with CO_2 stripping causes high pH variations. In its turn, pH affects the chemical equilibrium of substrates and inhibitory compounds. It is therefore essential to take up pH as a model variable. Nevertheless pH is not a state variable. Its concentration is not calculated from a mass balance (which would result in a differential equation) but from a charge balance over the reactor, expressing that the sum of all charges must be zero (Equation (1)).

$$\Delta_{ch} = [H^+] - [OH^-] + [NH_4^+] - [NO_2^-] - [NO_3^-] - [HCO_3^-] - 2\cdot[CO_3^{2-}] - [H_2PO_4^-] - 2\cdot[HPO_4^{2-}] + [Z^+] \quad (1)$$

In this equation, Z^+ represents the concentration of net positive charges which are not involved in chemical equilibrium reactions, and do not take part in biological conversions. Note that the concentration of Z^+ can be negative if there are more negative than positive charges. A detailed description of pH calculation by means of a charge balance can be found in Volcke *et al.* (2002).

MODEL CALIBRATION AND VALIDATION

Identifiability analysis

An identifiability analysis was performed to determine an identifiable subset of parameters to calibrate the model. For this purpose, 30 parameters (all kinetic parameters plus the temperature correction coefficients) have been considered, as well as five different outputs (NH_4^+, NO_2^-, NO_3^-, IC and pH).

First, the total sensitivity of each parameter, δ_j^{msqr}, was calculated, taking into account the sensitivity measures for all the outputs. High δ_j^{msqr} values imply high parameter significance. In this way, all parameters were ranked according to their importance. From this ranking, only the

more sensitive parameters could be considered identifiable. There is not a clear cut-off value for the δ_j^{msqr} (Ruano *et al.* 2007). Nevertheless, based on experience, a threshold value of 0.05 was chosen as a cut-off value to select the more significant parameters, and reduce the computational time for further collinearity index and determinant measures calculation. As a result, a subset containing the 12 parameters presenting the higher δ_j^{msqr} was selected.

Subsequently, the collinearity index (γ) and the determinant measures (ρ) for each output variable were calculated for all possible subsets containing two to 12 of the 12 most significant parameters. From these results, the larger parameter subsets satisfying the identifiability threshold (taken as $\gamma = 5$ in this study, based on previously reported experiences) were selected (see Table 3). Note that no subset is presented for NO_3^-, since no parameter subset yielded a collinearity index lower than the threshold value ($\gamma < 5$) for this output.

Calibration and validation

The calibration step was conducted in two stages, as proposed in Corominas (2006). First, the model was simulated with a constant influent to reach quasi steady-state, and the volatile suspended solids (VSS) concentration inside the reactor was adjusted by tuning the f_{ns}. Once achieved proper conditions, the cycle evolution calibration was performed following a step-wise procedure. The process dynamics were fitted by manually fine-tuning the identifiable parameter subsets previously found in the identifiability analysis (see Table 3). A maximum of 10% variation on the parameter, in respect to its default value, was considered acceptable. The model fitting to the respective output was visually assessed. In this sense, only μ_{max}^{AOB}, μ_{max}^{NOB} and pH_{opt} (accounting for the higher δ_j^{msqr} values) gave a significant response. The initial and final values of the tuned parameters are presented in Table 4.

Table 3 | Parameter subsets selected on the identifiability analysis

Output	Parameter subset	γ	ρ
NH_4^+	μ_{max}^{AOB}, μ_{max}^{NOB}, μ_{max}^{H}, b^H, K_{I,HNO_2}^{NOB}	4.77	3.5
NO_2^-	b^{AOB}, b^H, K_{SS}^H	4.23	8.57
IC	μ_{max}^{H}, η, b^{AOB}, b^H, K_{I,HNO_2}^{NOB}, pH_{opt}	4.28	120.50
pH	μ_{max}^{NOB}, μ_{max}^{HET}, η, b^{AOB}, b^H, K_{IC}, K_{SS}^H, K_{I,O_2}	4.7	1.29

Table 4 | Initial and calibrated values

Parameter	Initial	Calibrated
μ_{max}^{AOB}	2.1	2.31
μ_{max}^{NOB}	1.05	0.945
pH_{opt}	7.23	7.63

After finishing the calibration step, the model was validated using an independent data set, in this case cyclic profiles corresponding to step-feed operation (Figure 1). Figure 2 presents the results of the calibration (2.a, 2.b and 2.c) and the validation (2.d, 2.e and 2.f) for the nitrogen compounds, inorganic carbon and pH.

Figure 2 shows a good model fit to the data in both calibration and validation steps. The model accurately follows the dynamic trends in the nitrogen compounds (nitrite build-up, without nitrate production) and inorganic carbon. On the other hand, Figure 2(c,f) present the experimental and simulated pH profiles. As it can be seen, the model is capable of forecasting the pH dynamics, despite a slight bias (an off-set of about 0.3–0.4 pH units) between the simulated and experimental values. Taking into account the high sensitivity of pH in non-buffered systems, this deviation is deemed acceptable. One of the main hypotheses for this deviation may be the effect of salinity. Raw leachate used in this study presented a conductivity above 35,000 $\mu S\,cm^{-1}$. In this sense, elevated ionic strengths may affect pH calculation. Under such a high value, it is recommended to use activities instead of concentrations (Smith & Chen 2006).

Statistical tests for model evaluation

Besides the visual judgement described above, the model fit for the calibration and validation data sets was also quantified on the basis of statistical tests. Results are summarised in Table 5.

As can be seen in Table 5, ammonium and nitrite present MAE and RMSE values higher than 40. This is due to the elevated concentration of these compounds, and may not imply poor fittings. In this way, ARD could be useful to

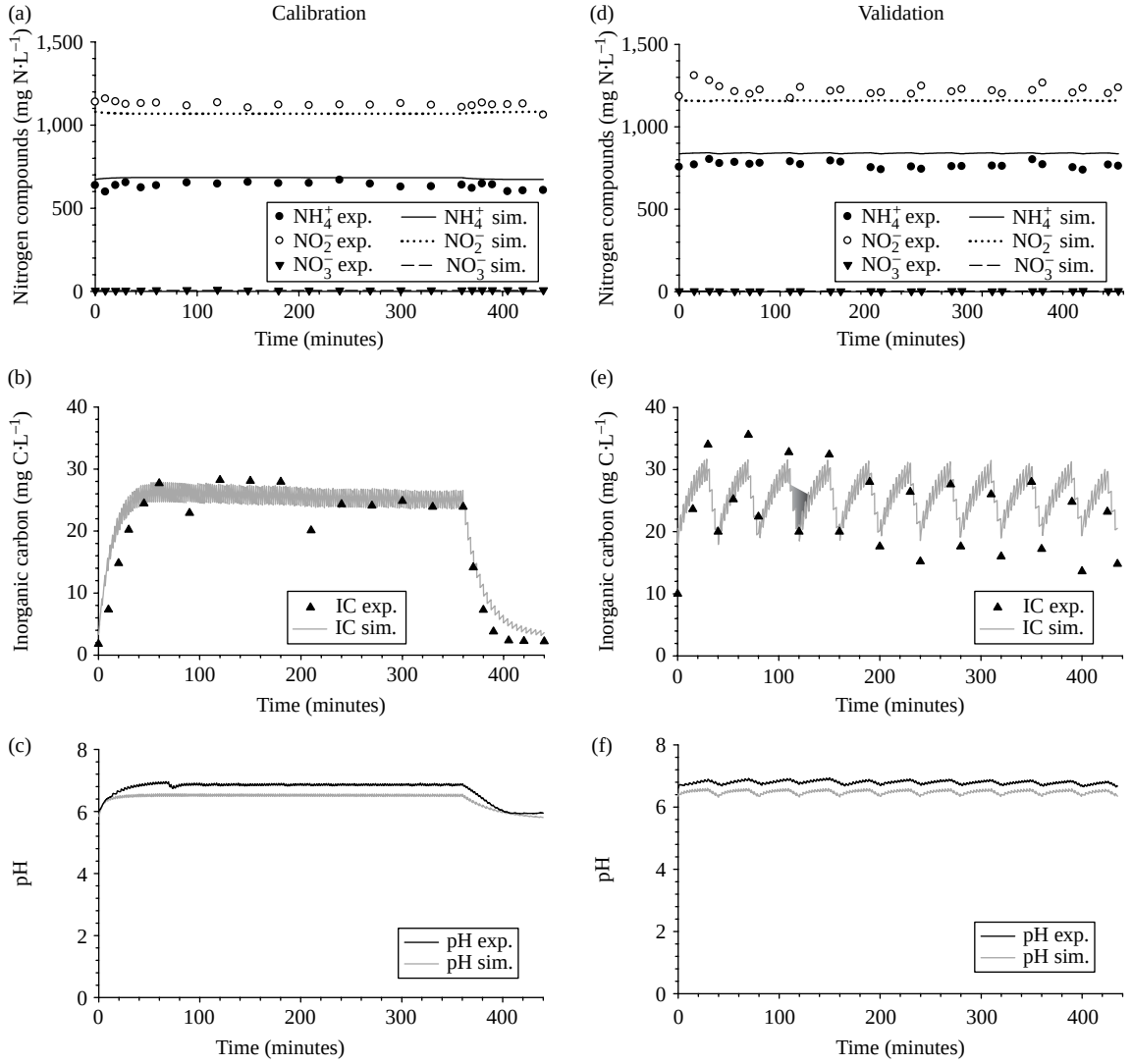

Figure 2 | Experimental and simulated evolution of the main physical-chemical outputs. Calibration step: (a) nitrogen compounds; (b) inorganic carbon; (c) pH. Validation step: (d) nitrogen compounds; (e) inorganic carbon; (f) pH.

Table 5 | Statistical tests

	MAE		RMSE		ARD		
Output	**Calibration**	**Validation**	**Calibration**	**Validation**	**Calibration**	**Validation**	J^2
NH_4^+	45.76	70.87	48.71	72.78	0.08	0.10	2.23
NO_2^-	52.83	64.76	54.43	70.96	0.05	0.06	1.70
NO_3^-	1.69	0.7	2.09	0.79	0.29	0.31	0.15
IC	2.80	3.42	3.43	4.15	0.53	0.27	1.47
pH	0.29	0.31	0.31	0.31	0.05	0.05	1.01

assess the adjustment of such concentrated compounds. Thus, average relative deviations of NH_4^+ and NO_2^- are lower than 10%, pointing out a good adjustment of the model to the experimental data. The higher values of these statistics for the validation could be related to the higher nitrogen concentration at the influent of the validation cycle (200–300 mg N-NH_4^+ L^{-1}). Regarding nitrate and inorganic carbon, both outputs present low MAE and RMSE values. On the contrary, the ARD statistic points out poor adjustments. Figure 2 has revealed a good fitting for the NO_3^- and IC; in this sense these high ARD values may be caused by a magnification of the deviation due to the low concentration of these compounds. Finally, results of the different statistics for the pH reveal a similar fitting on the calibration and validation step, presenting low MAE, RMSE and ARD values. Focusing on the Janus coefficient, values obtained for the PN-SBR model are not so far from 1, implying that the model structure has remained unchanged during calibration and validation periods. In this sense the predictive accuracy of the model has been verified.

CONCLUSIONS

A mathematical model of a partial nitrification SBR treating raw urban landfill leachate has been successfully constructed, calibrated and validated using historical data. The development of this model has been carried out following a systematic guideline, which has been upgraded through the inclusion of an identifiability analysis step as well as additional statistical tests for the evaluation of the model fitting.

The calibrated PN-SBR model is capable of predicting the behaviour of the main physical-chemical outputs (NH_4^+, NO_2^-, NO_3^- and IC) with a good accuracy. Good results were also obtained for pH, despite a slight bias on pH forecasting, probably caused by the high salinity of the leachate. In this way, the refinement on the prediction of this output should be taken into account for further model upgrading. Future work will be also addressed to the evaluation of the interaction of different factors (aeration, stripping, pH, inhibitions, among others) and their impact on the process.

ACKNOWLEDGEMENTS

The authors thank the Catalan Government (Postdoctoral fellowship "Beatriu de Pinós" BP-B1-00193-2007), CESPA-GR, the PANAMMOX project (CIT-310200-2007-90, PET-2006-0604) and the NOVEDAR CONSOLIDER project (CSD-2007-0055) for their financial support in this study. Also, the authors gratefully acknowledge the valuable contributions made by G. Rustullet and A. Cabezas during the experimental study. Eveline Volcke is a post-doctoral research fellow of the Research Foundation - Flanders (Belgium) (FWO).

REFERENCES

Brun, R., Kühni, M., Siegrist, H., Gujer, W. & Reichert, P. 2002 Practical identifiability of ASM2d parameters-systematic selection and tuning of parameter subsets. *Water Res.* **36**(16), 4113–4127.

Corominas, Ll. 2006 *Control and optimization of an SBR for nitrogen removal: From model calibration to plant operation*. PhD thesis, University of Girona, Girona, Spain. Available on: http://www.tesisenxarxa.net/TESIS_UdG/AVAILABLE/TDX-0720106-115017//tlct.pdf

Ganigué, R., López, H., Balaguer, M. D. & Colprim, J. 2007 Partial ammonium oxidation to nitrite of high ammonium content urban landfill leachates. *Water Res.* **41**(15), 3317–3326.

Ganigué, R., López, H., Ruscalleda, M., Balaguer, M. D. & Colprim, J. 2008 Operational strategy for a partial nitritation-SBR (PN-SBR) treating urban landfill leachate to achieve a stable influent for an anammox reactor. *J. Chem. Technol. Biotechnol.* **83**(3), 365–371.

Hellinga, C., van Loosdrecht, M. C. M. & Heijnen, J. J. 1999 Model based design of a novel process for nitrogen removal from concentrated flows. *Math. Comput. Model. Dyn. Syst.* **5**(4), 351–371.

Henze, M., Gujer, W., Mino, T. & van Loosdrecht, M. C. M. 2000 *Activated Sludge Models ASM1, ASM2, ASM2d and ASM3. Scientific and Technical Report*. IWA Publishing, London, UK, p. 121.

Lai, E., Senkpiel, S., Solley, D. & Keller, J. 2004 Nitrogen removal of high strength wastewater via nitritation/denitritation using a sequencing batch reactor. *Water Sci. Technol.* **50**(10), 27–33.

Lochtman, S. F. W. 1995 *Proceskeuze en -optimalisatie van het SHARON process voor slibverwerkingsbedrijf Sluisjesdijk (Process choice and optimisation of the SHARON process for the sludge treatment plant Sluisjesdijk)*. BODL report. TU Delft.

Magrí, A., Corominas, Ll., López, H., Campos, E., Balaguer, M. D., Colprim, J. & Flotats, X. 2007 A model for the simulation of the SHARON process: pH as a key factor. *Environ. Technol.* **28**(3), 255–265.

Muller, A., Wentzel, M. C., Loewenthal, R. E. & Ekama, G. A. 2003 Heterotroph anoxic yield in anoxic aerobic activated sludge systems treating municipal wastewater. *Water Res.* **37**, 2435–2441.

Power, M. 1993 The predictive validation of ecological and environmental models. *Ecol. Model.* **68**, 33–50.

Ruano, M. V., Ribes, J., De Pauw, D. J. W. & Sin, G. 2007 Parameter subset selection for the dynamic calibration of activated sludge models (ASMs): experience versus systems analysis. *Water Sci. Technol.* **56**(8), 107–115.

Sin, G., Kaelin, D., Kampschreur, M. J., Takács, I., Wett, B., Gernaey, K., Rieger, L., Siegrist, H. & van Loosdrecht, M. C. M. 2008 Modelling nitrite in wastewater treatment systems: a discussion of different modelling concepts. *Water Sci. Technol.* **58**(6), 1155–1171.

Smith, S. A. & Chen, S. 2006 Activity corrections for ionization constants in defined media. *Water Sci. Technol.* **54**(4), 21–29.

Van Dongen, U., Jetten, M. S. M. & van Loosdrecht, M. C. M. 2001 The SHARON-ANAMMOX process for treatment of ammonium rich wastewater. *Water Sci. Technol.* **44**(1), 153–160.

Van Hulle, S. W. H., Volcke, E. I. P., López-Teruel, J., Donckels, B., van Loosdrecht, M. C. M. & Vanrolleghem, P. A. 2007 Influence of temperature and pH on the kinetics of the SHARON nitritation process. *J. Chem. Technol. Biotechnol.* **82**(5), 471–480.

Volcke, E. I. P. 2006 *Modelling, analysis and control of partial nitritation in a SHARON reactor*. PhD thesis, Ghent University, Ghent, Belgium, p. 300. Available on: http://biomath.ugent.be/publications/download/VolckeEveline_PhD.pdf

Volcke, E. I. P., Hellinga, C., Van Den Broeck, S., van Loosdrecht, M. C. M. & Vanrolleghem, P. A. 2002 Modelling the SHARON process in view of coupling with Anammox. *Proceedings 1st IFAC International Scientific and Technical Conference on Technology, Automation and Control of Wastewater and Drinking Water Systems (TiASWiK'02)*. Gdansk-Sobieszewo, Poland, June 19–21 2002, pp. 65–72.

Wett, B. & Rauch, W. 2003 The role of inorganic carbon limitation in biological nitrogen removal of extremely ammonia concentrated wastewater. *Water Res.* **37**(5), 1100–1110.

Wiesmann U. 1994 *Advances in Biochemical Engineering/Biotechnology* (Vol. 51). Springer-Verlag, Berlin, Germany, pp. 113–154.

APPENDIX

Table A.1 | Stoichiometric matrix, including reaction rates

Process	S_{NH} gN m^{-3}	S_{NO_2} gN m^{-3}	S_{NO_3} gN m^{-3}	S_{N_2} gN m^{-3}	S_{IC} gC m^{-3}	S_{O_2} gO_2 m^{-3}	S_{IP} gP m^{-3}
Aerobic ammonium oxidation	$-\frac{1}{Y_{AOB}} - i_{NBM}$	$\frac{1}{Y_{AOB}}$	–	–	$-i_{CBM}$	$-\frac{3.43-Y_{AOB}}{Y_{AOB}}$	$-i_{PBM}$
Aerobic nitrite oxidation	$-i_{NBM}$	$-\frac{1}{Y_{NOB}}$	$\frac{1}{Y_{NOB}}$	–	$-i_{CBM}$	$-\frac{1.14-Y_{NOB}}{Y_{NOB}}$	$-i_{PBM}$
Aerobic organic matter oxidation	$\frac{1}{Y_H}\cdot i_{NSS} - i_{NBM}$	–	–	–	$\frac{1}{Y_H}\cdot i_{CSS} - i_{CBM}$	$-\frac{1-Y_H}{Y_H}$	$\frac{1}{Y_H}\cdot i_{PSS} - i_{PBM}$
Denitrification of nitrite	$\frac{1}{Y_{H,NO_2}}\cdot i_{NSS} - i_{NBM}$	$-\frac{1-Y_{H,NO_2}}{1.71\cdot Y_{H,NO_2}}$	–	$\frac{1-Y_{H,NO_2}}{1.71\cdot Y_{H,NO_2}}$	$\frac{1}{Y_{H,NO_2}}\cdot i_{CSS} - i_{CBM}$	–	$\frac{1}{Y_{H,NO_2}}\cdot i_{PSS} - i_{PBM}$
Denitrification of nitrate	$\frac{1}{Y_{H,NO_3}}\cdot i_{NSS} - i_{NBM}$	$\frac{1-Y_{H,NO_3}}{1.14\cdot Y_{H,NO_3}}$	$-\frac{1-Y_{H,NO_3}}{1.14\cdot Y_{H,NO_3}}$	–	$\frac{1}{Y_{H,NO_3}}\cdot i_{CSS} - i_{CBM}$	–	$\frac{1}{Y_{H,NO_3}}\cdot i_{PSS} - i_{PBM}$
Hydrolysis of X_S	$i_{NXS} - i_{NSS}$	–	–	–	$i_{CXS} - i_{CSS}$	–	$i_{PXS} - i_{PSS}$
Aerobic endogenous respiration of X_{AOB}	$i_{NBM} - fx_I\cdot i_{NXI}$	–	–	–	$i_{CBM} - fx_I\cdot i_{CXI}$	$-(1-fx_I)$	$i_{PBM} - fx_I\cdot i_{PXI}$
Anoxic endogenous respiration of X_{AOB} on NO_3^-	$i_{NBM} - fx_I\cdot i_{NXI}$	$\frac{1-fx_I}{1.14}$	$-\frac{1-fx_I}{1.14}$	–	$i_{CBM} - fx_I\cdot i_{CXI}$	–	$i_{PBM} - fx_I\cdot i_{PXI}$
Anoxic endogenous respiration of X_{AOB} on NO_2^-	$i_{NBM} - fx_I\cdot i_{NXI}$	$-\frac{1-fx_I}{1.71}$	–	$\frac{1-fx_I}{1.71}$	$i_{CBM} - fx_I\cdot i_{CXI}$	–	$i_{PBM} - fx_I\cdot i_{PXI}$
Aerobic endogenous respiration of X_{NOB}	$i_{NBM} - fx_I\cdot i_{NXI}$	–	–	–	$i_{CBM} - fx_I\cdot i_{CXI}$	$-(1-fx_I)$	$i_{PBM} - fx_I\cdot i_{PXI}$
Anoxic endogenous respiration of X_{NOB} on NO_3^-	$i_{NBM} - fx_I\cdot i_{NXI}$	$\frac{1-fx_I}{1.14}$	$-\frac{1-fx_I}{1.14}$	–	$i_{CBM} - fx_I\cdot i_{CXI}$	–	$i_{PBM} - fx_I\cdot i_{PXI}$
Anoxic endogenous respiration of X_{NOB} on NO_2^-	$i_{NBM} - fx_I\cdot i_{NXI}$	$-\frac{1-fx_I}{1.71}$	–	$\frac{1-fx_I}{1.71}$	$i_{CBM} - fx_I\cdot i_{CXI}$	–	$i_{PBM} - fx_I\cdot i_{PXI}$
Aerobic endogenous respiration of X_H	$i_{NBM} - fx_I\cdot i_{NXI}$	–	–	–	$i_{CBM} - fx_I\cdot i_{CXI}$	$-(1-fx_I)$	$i_{PBM} - fx_I\cdot i_{PXI}$
Anoxic endogenous respiration of X_H on NO_3^-	$i_{NBM} - fx_I\cdot i_{NXI}$	$\frac{1-fx_I}{1.14}$	$-\frac{1-fx_I}{1.14}$	–	$i_{CBM} - fx_I\cdot i_{CXI}$	–	$i_{PBM} - fx_I\cdot i_{PXI}$
Anoxic endogenous respiration of X_H on NO_2^-	$i_{NBM} - fx_I\cdot i_{NXI}$	$-\frac{1-fx_I}{1.71}$	–	$\frac{1-fx_I}{1.71}$	$i_{CBM} - fx_I\cdot i_{CXI}$	–	$i_{PBM} - fx_I\cdot i_{PXI}$

Process	X_{AOB} g COD m^{-3}	X_{NOB} g COD m^{-3}	X_H g COD m^{-3}	S_S g COD m^{-3}	X_S g COD m^{-3}	X_I g COD m^{-3}	Process rates
Aerobic ammonium oxidation	1	–	–	–	–	–	$\mu_{max}^{AOB}\cdot\frac{S_{NH_3}}{K_{NH_3}^{AOB}+S_{NH_3}}\cdot\frac{S_{O_2}}{K_{O_2}^{AOB}+S_{O_2}}\cdot\frac{K_{I,NH_3}^{AOB}}{K_{I,NH_3}^{AOB}+S_{NH_3}}\cdot\frac{K_{I,HNO_2}^{AOB}}{K_{I,HNO_2}^{AOB}+S_{HNO_2}}\cdot\frac{S_{HCO_3^-}}{K_{HCO_3^-}+S_{HCO_3^-}}\cdot\frac{K_{pH}}{K_{pH}-1+10^{\lvert pH_{opt}-pH\rvert}}\cdot X_{AOB}$
Aerobic nitrite oxidation	–	1	–	–	–	–	$\mu_{max}^{NOB}\cdot\frac{S_{HNO_2}}{K_{HNO_2}^{NOB}+S_{HNO_2}}\cdot\frac{S_{O_2}}{K_{O_2}^{NOB}+S_{O_2}}\cdot\frac{K_{I,HNO_2}^{NOB}}{K_{I,HNO_2}^{NOB}+S_{HNO_2}}\cdot\frac{K_{I,NH_3}^{NOB}}{K_{I,NH_3}^{NOB}+S_{NH_3}}\cdot\frac{S_{HCO_3^-}}{K_{HCO_3^-}+S_{HCO_3^-}}\cdot\frac{K_{pH}}{K_{pH}-1+10^{\lvert pH_{opt}-pH\rvert}}\cdot X_{NOB}$
Aerobic organic matter oxidation	–	–	1	$-\frac{1}{Y_H}$	–	–	$\mu_{max}^{H}\cdot\frac{S_{O_2}}{K_{O_2}^{H}+S_{O_2}}\cdot\frac{S_S}{K_{S_S}^{H}+S_S}\cdot\frac{K_{pH}}{K_{pH}-1+10^{\lvert pH_{opt}-pH\rvert}}\cdot X_H$
Denitrification of nitrite	–	–	1	$-\frac{1}{Y_{H,NO_2}}$	–	–	$\mu_{max}^{H}\cdot\eta\cdot\frac{S_{NO_2}}{K_{NO_2}^{dNO_2}+S_{NO_2}}\cdot\frac{S_S}{K_{S_S}^{H}+S_S}\cdot\frac{S_{NO_2}}{S_{NO_3}+S_{NO_2}}\cdot\frac{K_{I,O_2}}{K_{I,O_2}+S_{O_2}}\cdot\frac{K_{pH}}{K_{pH}-1+10^{\lvert pH_{opt}-pH\rvert}}\cdot X_H$

Table A.1 | (*continued*)

Process	X_{AOB} g COD m^{-3}	X_{NOB} g COD m^{-3}	X_H g COD m^{-3}	S_S g COD m^{-3}	X_S g COD m^{-3}	X_I g COD m^{-3}	Process rates
Denitrification of nitrate	–	–	1	$-\frac{1}{Y_{H,NO_3}}$	–	–	$\mu_{max}^{H}\cdot\eta\cdot\frac{S_{NO_3}}{K_{NO_3}^{dNO_3}+S_{NO_3}}\cdot\frac{S_S}{K_{S_S}^{H}+S_S}\cdot\frac{S_{NO_3}}{S_{NO_3}+S_{NO_2}}\cdot\frac{K_{I,O_2}}{K_{I,O_2}+S_{O_2}}\cdot\frac{K_{pH}}{K_{pH}-1+10^{\lvert pH_{opt}-pH\rvert}}\cdot X_H$
Hydrolysis of X_S	–	–	–	1	−1	–	$K_H\cdot\frac{X_S/X_H}{K_X+X_S/X_H}\cdot X_H$
Aerobic endogenous respiration of X_{AOB}	−1	–	–	–	–	fx_I	$b_{AOB}\cdot\frac{S_{O_2}}{K_{O_2}^{AOB}+S_{O_2}}\cdot X_{AOB}$
Anoxic endogenous respiration of X_{AOB} on NO_3^-	−1	–	–	–	–	fx_I	$b_{AOB}\cdot\eta\cdot\frac{K_{I,O_2}}{K_{I,O_2}+S_{O_2}}\cdot\frac{S_{NO_3}}{K_{NO_3}+S_{NO_3}}\cdot\frac{S_{NO_3}}{S_{NO_3}+S_{NO_2}}\cdot X_{AOB}$
Anoxic endogenous respiration of X_{AOB} on NO_2^-	−1	–	–	–	–	fx_I	$b_{AOB}\cdot\eta\cdot\frac{K_{I,O_2}}{K_{I,O_2}+S_{O_2}}\cdot\frac{S_{NO_2}}{K_{NO_2}+S_{NO_2}}\cdot\frac{S_{NO_2}}{S_{NO_3}+S_{NO_2}}\cdot X_{AOB}$
Aerobic endogenous respiration of X_{NOB}	–	−1	–	–	–	fx_I	$b_{NOB}\cdot\frac{S_{O_2}}{K_{O_2}^{NOB}+S_{O_2}}\cdot X_{NOB}$
Anoxic endogenous respiration of X_{NOB} on NO_3^-	–	−1	–	–	–	fx_I	$b_{NOB}\cdot\eta\cdot\frac{K_{I,O_2}}{K_{I,O_2}+S_{O_2}}\cdot\frac{S_{NO_3}}{K_{NO_3}+S_{NO_3}}\cdot\frac{S_{NO_3}}{S_{NO_3}+S_{NO_2}}\cdot X_{NOB}$
Anoxic endogenous respiration of X_{NOB} on NO_2^-	–	−1	–	–	–	fx_I	$b_{NOB}\cdot\eta\cdot\frac{K_{I,O_2}}{K_{I,O_2}+S_{O_2}}\cdot\frac{S_{NO_2}}{K_{NO_2}+S_{NO_2}}\cdot\frac{S_{NO_2}}{S_{NO_3}+S_{NO_2}}\cdot X_{NOB}$
Aerobic endogenous respiration of X_H	–	–	−1	–	–	fx_I	$b_H\cdot\frac{S_{O_2}}{K_{O_2}^{H}+S_{O_2}}\cdot X_H$
Anoxic endogenous respiration of X_H on NO_3^-	–	–	−1	–	–	fx_I	$b_H\cdot\eta\cdot\frac{K_{I,O_2}}{K_{I,O_2}+S_{O_2}}\cdot\frac{S_{NO_3}}{K_{NO_3}+S_{NO_3}}\cdot\frac{S_{NO_3}}{S_{NO_3}+S_{NO_2}}\cdot X_H$
Anoxic endogenous respiration of X_H on NO_2^-	–	–	−1	–	–	fx_I	$b_H\cdot\eta\cdot\frac{K_{I,O_2}}{K_{I,O_2}+S_{O_2}}\cdot\frac{S_{NO_2}}{K_{NO_2}+S_{NO_2}}\cdot\frac{S_{NO_2}}{S_{NO_3}+S_{NO_2}}\cdot X_H$

Table A.2 | Stoichiometric parameters

Symbol	Definition	Value	Units	Reference
Y_{AOB}	Yield of ammonia oxidation	0.15	g COD (g N)$^{-1}$	Wiesmann (1994)
Y_{NOB}	Yield of nitrite oxidation	0.041	mg COD (g N)$^{-1}$	Wiesmann (1994)
Y_H	Yield of aerobic organic matter oxidation	0.67	g COD (g COD)$^{-1}$	Henze *et al.* (2000); ASM1
Y_{H,NO_2}	Yield of denitrification via nitrite	0.53	g COD (g COD)$^{-1}$	adapted from Muller *et al.* (2003)
Y_{H,NO_3}	Yield of denitrification via nitrate	0.53	g COD (g COD)$^{-1}$	Muller *et al.* (2003)
i_{NBM}	Nitrogen content of the biomass	0.070	g N (g COD)$^{-1}$	Henze *et al.* (2000); ASM3
i_{PBM}	Phosphorus content of the biomass	0.021	g P (g COD)$^{-1}$	Volcke (2006)
i_{CBM}	Carbon content of the biomass	0.36	g C (g COD)$^{-1}$	Volcke (2006)
i_{NXS}	Nitrogen content of X_S	0.04	g N (g COD)$^{-1}$	Henze *et al.* (2000); ASM3
i_{PXS}	Phosphorus content of X_S	0.0089	g P (g COD)$^{-1}$	Volcke (2006)
i_{CXS}	Carbon content of X_S	0.3	g C (g COD)$^{-1}$	Volcke (2006)
i_{NSS}	Nitrogen content of S_S	0.03	g N (g COD)$^{-1}$	Henze *et al.* (2000); ASM3
i_{PSS}	Phosphorus content of S_S	0.0089	g C (g COD)$^{-1}$	Volcke (2006)
i_{CSS}	Carbon content of S_S	0.3	g C (g COD)$^{-1}$	Volcke (2006)
fx_I	Production of X_I in endogenous respiration	0.08	g COD (g COD)$^{-1}$	Henze *et al.* (2000); ASM1
i_{NXI}	Nitrogen fraction in X_I	0.02	g N (g COD)$^{-1}$	Henze *et al.* (2000); ASM3
i_{PXI}	Phosphorus fraction in X_I	0.00064	g P (g COD)$^{-1}$	Volcke (2006)
i_{CXI}	Carbon fraction in X_I	0.36	g C (g COD)$^{-1}$	Volcke (2006)

Table A.3 | Kinetic parameters

Symbol	Characterization	Value (T = 35°C)	Units	Reference
μ_{max}^{AOB}	Maximum growth rate AOB	2.1	d^{-1}	Lochtman (1995)
b^{AOB}	Aerobic endogenous respiration rate for AOB	0.1944	d^{-1}	Wiesmann (1994)
$K_{NH_3}^{AOB}$	Ammonia substrate saturation for AOB	0.75	$g\,N\,m^{-3}$	Van Hulle *et al.* (2007)
$K_{O_2}^{AOB}$	Oxygen substrate saturation for AOB	0.3	$g\,N\,m^{-3}$	Wiesmann (1994)
K_{I,NH_3}^{AOB}	Free ammonia inhibition constant for AOB	605.48	$g\,N\,m^{-3}$	Ganigué *et al.* (2007)
K_{I,HNO_2}^{AOB}	Nitrous acid inhibition constant for AOB	0.49	$g\,N\,m^{-3}$	Ganigué *et al.* (2007)
$K_{HCO_3^-}$	Inorganic carbon substrate saturation	0.01	$g\,C\,m^{-3}$	Ganigué *et al.* (2007)
K_{pH}	Saturation constant for pH	8.21	–	Van Hulle *et al.* (2007)
pH_{opt}	Optimum pH	7.23	–	Van Hulle *et al.* (2007)
μ_{max}^{NOB}	Maximum growth rate NOB	1.05	d^{-1}	Lochtman (1995)
b^{NOB}	Aerobic endogenous respiration rate for NOB	0.0795	d^{-1}	Wiesmann (1994)
$K_{HNO_2}^{NOB}$	Nitrite substrate saturation for NOB	3.2×10^{-5}	$g\,N\,m^{-3}$	Wiesmann (1994)
$K_{O_2}^{NOB}$	Oxygen substrate saturation for NOB	1.1	$g\,O_2\,m^{-3}$	Wiesmann (1994)
K_{I,HNO_2}^{NOB}	Nitrous acid inhibition constant for NOB	0.26	$g\,N\,m^{-3}$	Wiesmann (1994)
$K_{I,NH3}^{NOB}$	Free ammonia inhibition constant for NOB	14.8	$g\,N\,m^{-3}$	Magrí *et al.* (2007)
μ_{max}^{H}	Maximum growth rate for heterotrophic biomass	16.97	d^{-1}	Henze *et al.* (2000); ASM1
b^{H}	Aerobic endogenous respiration rate for heterotrophic biomass	3.18	d^{-1}	Henze *et al.* (2000); ASM1
$K_{O_2}^{H}$	Oxygen saturation for heterotrophic biomass	0.2	$g\,O_2\,m^{-3}$	Henze *et al.* (2000); ASM1
K_{SS}	Substrate saturation for heterotrophic biomass	20	$g\,COD\,m^{-3}$	Henze *et al.* (2000); ASM1
$K_{NO_2}^{dNO_2}$	Nitrite substrate saturation for nitrite denitrifiers	0.119	$g\,N\,m^{-3}$	Wiesmann (1994)
$K_{NO_3}^{dNO_3}$	Nitrate substrate saturation for nitrate denitrifiers	0.14	$g\,N\,m^{-3}$	Wiesmann (1994)
K_{NO_2}	Saturation constant of SNO_2 for endogenous respiration	0.5	$g\,N\,m^{-3}$	Henze *et al.* (2000); ASM1
K_{NO_3}	Saturation constant of SNO_3 for endogenous respiration	0.5	$g\,N\,m^{-3}$	Henze *et al.* (2000); ASM1
K_{I,O_2}	Oxygen inhibition constant for denitrifiers	0.20	$g\,O_2\,m^{-3}$	Henze *et al.* (2000); ASM1
η	Anoxic reduction factor	0.6	–	Henze *et al.* (2000); ASM3
K_H	Maximum specific hydrolysis rate	15.59	$g\,COD\,(g\,COD\,d)^{-1}$	Henze *et al.* (2000); ASM1
K_X	Saturation constant for slowly biodegradable substrate	0.1559	$g\,COD\,g\,COD^{-1}$	Henze *et al.* (2000); ASM1

Table A.4 | Temperature correction factors

Symbol	Characterization	Value ($°C^{-1}$)
θ^{AOB}	Theta value for AOB	0.086
θ^{NOB}	Theta value for NOB	0.056
θ^{H}	Theta value for heterotrophic organisms	0.104